Divergent and Convergent Forms of a New Schiff-base Cryptand; X-Ray Crystallographic and Molecular Mechanics Investigations *

Michael G. B. Drew,[a] Debbie Marrs,[b,c] Josie Hunter[b,c] and Jane Nelson[b,c]
[a] *Department of Chemistry, The University, Whiteknights, Reading RG6 2AD, UK*
[b] *School of Chemistry, The Queen's University of Belfast, Belfast BT9 5AG, UK*
[c] *Open University, 40 University Road Belfast BT7 1SU, UK*

A hexaimino cryptand L^1 has been obtained by condensation of tris(2-aminoethyl)amine with terephthalaldehyde without template. An X-ray crystal structure determination has been carried out on $L^1 \cdot 6H_2O$ and shows a divergent conformation for the macrocycle in which all six imine nitrogen atoms form hydrogen bonds to water molecules positioned outside the macrobicycle. In the presence of Cu^I and Ag^I a convergent form of the macrocycle which allows encapsulation of a pair of cations is adopted. Tetra- and di-thiocyanato derivatives $[M_2L^1(NCS)_x(ClO_4)_y]$ ($x = 2$ or 4, $y = 2$ or 0) have also been prepared with M = Co, Ni or Cu. In these molecules the thiocyanate ligand adopts a terminal rather than bridging mode. Molecular mechanics and molecular dynamics calculations indicate that at least four different conformations of L^1 are likely to be found. Conformational preferences of L^1 have been established in the gas phase, in water and in the presence of metal ions.

The incorporation of the tripodal skeleton deriving from $N[(CH_2)_nX]_3$ (X = OH or NH_2) into binucleating macrobicyclic ligands was achieved many years ago by Lehn and co-workers.[1] A great deal of important work has followed on the exploitation of these cryptands[2,3] demonstrating their value as host molecules for ionic guests, both anions and cations, including pairs of transition ions. Some of these macrobicyclic ligands make use of O-donors, which are particularly suited to the accommodation of the 'harder' main group cations, while others incorporate saturated amino donors which can co-ordinate the 'softer' transition ions. In order fully to exploit the potential of the macrobicyclic framework, it seems appropriate to investigate transition-metal complexes of cryptands incorporating the sp^2-N donors which are of value in stabilizing the low oxidation states of interest in many examples of redox catalysis.

The Schiff-base condensation reaction has been used to generate a large number of ligands which have been widely exploited in transition-metal chemistry. Thus, [1 + 2] condensation of *e.g.* dicarbonyls with monoamines gives rise to acyclic ligands[4] while [1 + 1] or [2 + 2] condensation of dicarbonyls with diamines generates macrocyclic ligands;[5] those from the 'double' [2 + 2] condensation frequently function as binucleating ligands. Recently the Schiff-base condensation strategy has been extended[6,7] *via* use of triamines in place of diamines to generate macrobicycles (*via* [2 + 3] condensation of a triamine with a dicarbonyl) in place of macrocycles. The resulting Schiff-base cryptands are potentially binucleating ligands with N_4-donor site separation of up to 11 Å. The present study describes the ligand, L^1, obtained as the hexahydrate **1** by [2 + 3] condensation of tris(2-aminoethyl)amine (tren) with terephthalaldehyde, which contains a well separated (at 4–6 Å) pair of N_4 co-ordination sites consisting of three relatively soft imino-donors and one bridgehead tertiary amino nitrogen. Separation of the sites depends to some extent on whether the bridgehead

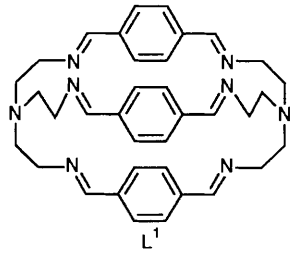

L^1

N is bonded to the metal, but the maximum separation can be set at 6.06 Å by reference to the Ag···Ag distance in $[Ag_2L^1]^{2+}$ which has been structurally characterized by X-ray crystallography.[8]

The degree of steric protection afforded the co-ordinated metal ion or other guest depends on the orientation of the aromatic rings relative to each other; thus conformational factors are expected to play an important part in host–guest relationships in such macrobicyclic cyclophane systems. While good steric protection is an objective of importance for some applications, for others easy access to the co-ordination site takes priority. The structural and molecular mechanics investigations described below address the question of conformational preferences and mobility in the ligand.

Results and Discussion

The capacity of L^1 to adopt a convergent configuration has already been demonstrated by means of its synthesis upon a disilver template. The X-ray crystallographic structure determination[8] of $[Ag_2L^1][CF_3SO_3]_2$ **2** reveals, in addition to the 6.06 Å separation of Ag^+ ions already mentioned, a trigonal arrangement of aromatic rings with respect to the C_3 axis, which passes through the bridgehead nitrogen atoms. In this conformation the aromatic CH groups make a closer than expected approach to Ag^+ which possibly signifies a weak bonding interaction particularly as molecular mechanics modelling suggests it may be avoidable (by allowing the macrobicycle to relax by stretching along the symmetry axis).

* *Supplementary data available:* see Instructions for Authors, *J. Chem. Soc., Dalton Trans.*, 1992, Issue 1, pp. xx–xxv.
Non-SI units employed: cal = 4.184 J, D ≈ 3.33 × 10^{-30} C m.

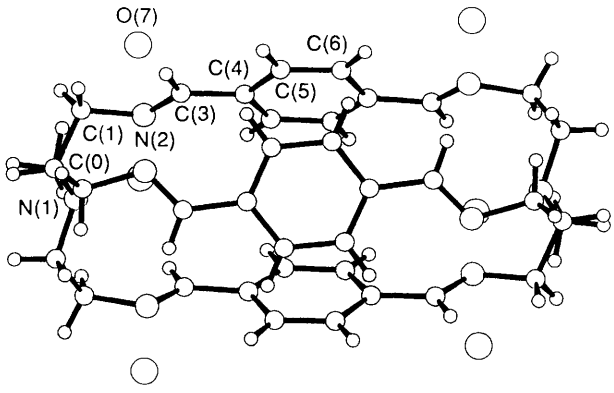

Fig. 1 The structure of $L^1 \cdot 6H_2O$ **1**. Hydrogen atoms on the water molecules are omitted for clarity

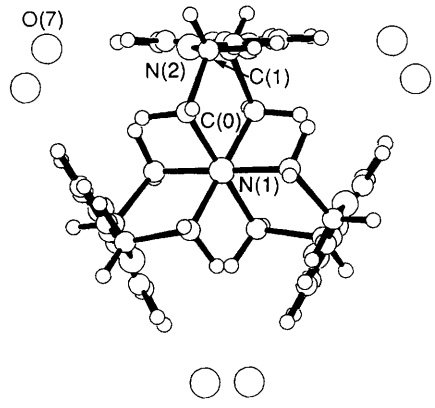

Fig. 2 The structure of $L^1 \cdot 6H_2O$ **1** looking down the N(bridgehead) ··· N(bridgehead) vector. Hydrogen atoms on the water molecules are omitted for clarity

Table 1 Details of hydrogen bonds (Å) in $L^1 \cdot 6H_2O$

N(4) ··· O(4) (x, y, z)*	2.95(1)
O(4) ··· O(4) ($\frac{1}{3} + y, x - \frac{1}{3}, -\frac{1}{3} - z$)	2.79(1)
O(4) ··· O(4) ($x - y, -y, -z$)	2.86(1)

* Symmetry element of second atom.

The trigonal disposition of aromatic rings in this conformation allows for good access to the co-ordination site, while steric protection is only moderate. Other conformations are of course available to the macrobicycle, which makes the X-ray structure of the free ligand, L^1, obtained by non-template synthesis, of particular interest.

The ligand was obtained in good yield as the hexahydrate, $L^1 \cdot 6H_2O$,[1] *via* condensation of tren and terephthalaldehyde in a methanol–acetonitrile solvent mixture at ambient temperature. Our initial observation of strong ν_{OH} absorption in the infrared and ^1H NMR spectra led us to believe that water might be encapsulated as a guest within the cavity. However this did not prove to be the case and the conformation in the free cryptand is very different from that in the disilver cryptate.

The Structure of Compound **1**.—The structure of compound **1** consists of discrete macrobicycles L^1 together with six water molecules. The macrocycle has imposed crystallographic 32 symmetry. A general view of the structure is shown in Fig. 1, while Fig. 2 shows a projection down the N(bridgehead) ··· N(bridgehead) vector.

Thus the six water molecules are outside the macrobicycle; each one forms a hydrogen bond to a nitrogen atom [O ··· N 2.95(1) Å]. In addition each water molecule is hydrogen-bonded to two of the others and therefore links macrobicycles (Table 1).

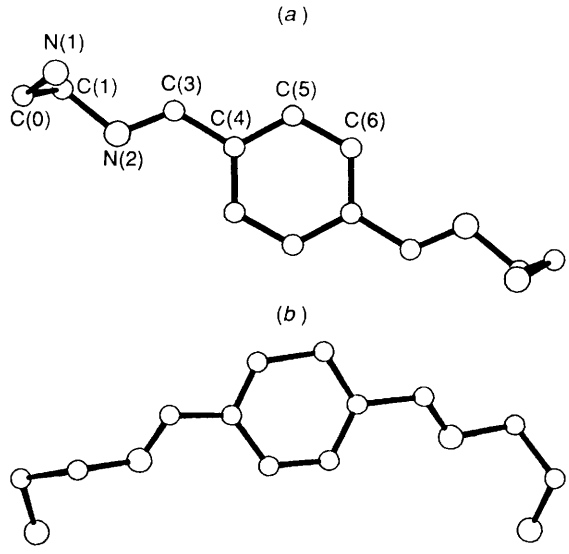

Fig. 3 A comparison of the different conformations of the macrocycle L^1 in the two structures (*a*) $L^1 \cdot 6H_2O$ **1** and (*b*) $[Ag_2L^1]^{2+}$ **2**. In both structures all three links are equivalent and for clarity only one link is shown

The conformation of the macrocycle is strikingly different from that found in $[Ag_2L^1]^{2+}$ (ref. 8) where the two silver atoms are encapsulated within the macrocycle and each bonded to four nitrogen atoms. In that complex the lone pairs on the imine nitrogen atoms were necessarily pointing towards the metal atom. In the present structure of the free macrocycle these lone pairs on the nitrogen atoms are pointing outwards towards the water molecules. These different conformations are compared in Fig. 3.

Molecular Mechanics Calculations.—Possible conformations of L^1 were investigated *via* computer modelling techniques. We used the two known crystal structures namely $[Ag_2L^1]^{2+}$ **2** and $L^1 \cdot 6H_2O$ **1** as starting models. As can be seen from Fig. 3 there are several conformational differences in the macrocycle between the two structures. The most significant difference is in the mutual arrangement of the C=N bonds relative to the phenyl rings. There are two possible arrangements, which we describe as **s** (nitrogen atoms on the same side of the phenyl ring) and **o** (nitrogen atoms on opposite sides of the phenyl ring) respectively. We can thus describe the two structures: $[Ag_2L^1]^+$

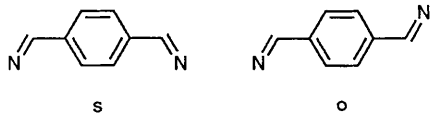

s o

has the **sss** conformation and $L^1 \cdot 6H_2O$ has the **ooo** conformation. These two symmetrical conformations can also be described as convergent (**sss**) and divergent (**ooo**). We used the molecular graphics system INSIGHT/DISCOVER[9] to build four conformations of L^1: **sss**, **sso**, **soo** and **ooo**; **sss** and **ooo** were taken from the crystal structures with extraneous atoms (metal ions, anions, solvent) removed, and **sso** and **soo** were constructed from **s** and **o** fragments. These four conformations were then investigated using the MM2MX program.[10] All force-field parameters were available in the program or could be easily derived except for the N=C–C_{ar}–C_{ar} and N=C–C_{ar}–H torsion angles. In the program, the torsion-angle energy is described by $0.5V_1(1 + \cos \alpha) + 0.5V_2(1 - \cos 2\alpha) + 0.5V_3(1 + \cos 3\alpha)$, where α is the torsion angle. We set V_1 and V_3 to 0.0 kcal mol^{-1} and so the value given to the V_2 parameter is a measure of conjugation in the N=C–Ph linkage. The experimental value of

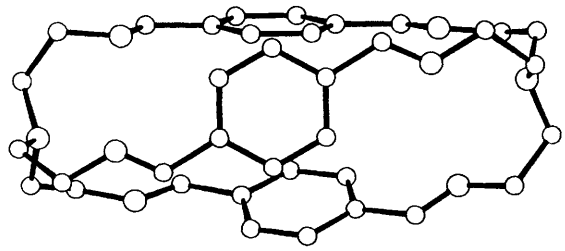

Fig. 4 The structure of the conformation **soo** of L^1 as established by molecular mechanics

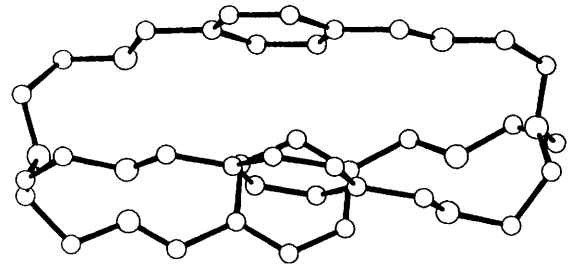

Fig. 5 The structure of conformation **sso** of L^1 as established by molecular mechanics

Table 2 Charge dipoles used in the MM2MX program for L^1

Bond	Charge difference (e) calculated from MOPAC	Bond length (Å)	Bond dipole (D)[a]
$C(sp^3)$–$N(sp^3)$	0.54	1.48	1.79
$C(sp^3)$–$N(sp^2)$	0.39	1.42	1.24
$C(sp^2)$–$N(sp^2)$	0.42	1.24	1.17
$C(sp^2)$–H	−0.11	1.08	0.27
$C(sp^2)$–C(ar)	0.18	1.46	0.59
$C(sp^3)$–H	−0.15	1.08	0.36
O–H			−1.15[b]
O–LP[c]			0.90[b]
N–LP			0.76[b]

[a] Bond dipole = $2.24r_{ij}(q_i - q_j)$. In $[H_2L^1]^{2+}$ the bond dipoles for C–N(sp^3) and N–H were set to 0.12 and −0.45D respectively. [b] Taken from the MM2(87) force field. [c] Lp = lone pair.

these torsion angles is only 2.6° in L^1, but 21° in $[Ag_2L^1]^{2+}$.[8] After some experimentation, we found that a value of 1.5 kcal mol^{-1} for V_2 was suitable and indeed reproduced well the experimental structure of the **ooo** conformation.

Molecular mechanics optimization on our four initial structures gave respective energies (kcal mol^{-1}) of **sss** (19.86), **sso** (38.78), **soo** (30.87) and **ooo** (22.45). In our search for energy minima for L^1 we confined ourselves to just these four conformations. However there were several other possible structures for each conformation that could arise *via* variations in the saturated region of the macrocycle around the bridgehead nitrogen atoms and it proved difficult to investigate all possibilities just using molecular graphics. We therefore carried out a conformational search procedure using molecular dynamics and the INSIGHT/DISCOVER software[9] on a Silicon Graphics Personal Iris Workstation. Details of this procedure are described below in the section headed molecular dynamics.

While rotation around the N=C–C_{ar}–C_{ar} torsion angle was infrequent, changes in conformation around the bridgehead nitrogen atom occurred much more readily and several variations were found in the **sso** and **soo** structures. The lowest-energy conformations were different from those set up in the crude starting models. These new conformations of the **sso** and **ooo** structures were then minimised using the MM2MX program* and we found energies for **soo** of 22.66 kcal mol^{-1} and for **sso** of 31.80 kcal mol^{-1}. We were unable to find any different conformations for the **sss** and **ooo** structures (which had energies of 19.86 and 22.45 kcal mol^{-1}), so the conformational order of preference of the four conformations in the gas phase was **sss** > **ooo**, **soo** > **sso**. The structures of the **soo** and **sso** conformations are shown in Figs. 4 and 5.

However the MM2MX force field used for these calculations did not include coulombic terms. Our experience and that of others has shown that charges are necessary for many applications of molecular mechanics, particularly when interactions between molecules are concerned. We therefore adopted a recognized technique by obtaining charges from a quantum mechanics calculation and including them in the molecular mechanics force field. We ran the four molecules through the semiempirical quantum mechanics program MOPAC[11] and abstracted the charges on the atoms. These were then turned into bond dipoles using an algorithm (1) due to Damewood

$$\text{bond dipole} = 2.24r_{ij}(q_i - q_j) \quad (1)$$

et al[12] for crown ether calculations and applied by us previously to calculations on 1,4,7,10,13,16-hexaazacyclooctadecane.[13] The scaling factor of 2.24 in equation (1) was derived in order to fit differences in energies for 18-crown-6 conformations to experimental data. The charge dipoles in the molecules obtained by this method and added to the force field MM2MX are listed in Table 2. We also included lone pairs on the nitrogen atoms in the calculation as suggested by Allinger.[14] The resulting absolute energies were much increased and the relative energies of the conformations were very different from those when no charges were employed. Results are compared in Table 3. When charges are included the **ooo** conformation has the lowest energy and the **sss** has the highest energy. Heats of formation were calculated using the PM3 parameterization[15] of the MOPAC semiempirical quantum-mechanics program. The order of preference **ooo** > **soo** > **sso** > **sss** is comparable with that for the molecular mechanics values.

Molecular Dynamics Calculations.—Calculations were carried out using the INSIGHT/DISCOVER software;[9] first to carry out a conformational search and secondly to study interconversions between the conformations. The dynamics was initiated for the four conformations **sss**, **sso**, **soo**, **ooo** in turn at 300 K with a step size of 1 fs and continued for 50 ps. During the run after each 1000 steps (1 ps) the structure was saved. Charges were included on the atoms as obtained from MOPAC 5.0.[11] At the end of each run the 50 structures obtained were recalled and minimized using molecular mechanics. By studying the resulting structures and energies, we obtained lower-energy conformations for the **sso** and **soo** conformations (see above) for use in the molecular mechanics calculations.

The molecular dynamics results (Table 4) were also used to investigate the interconversion of the various conformations. The **sss** conformation was never observed and the **sso** conformation was only once observed. The **soo** and **ooo** conformations were observed in a ratio of *ca.* 1:4. This

* A referee has questioned our use of INSIGHT/DISCOVER for molecular dynamics calculations and MM2MX (with a different force field) for molecular mechanics. We agree that this approach is not ideal (and it is certainly time-consuming) but argue that it is logical and makes the best use of the software available to us when this work was done. Our reasoning is that the MM2 force field is the best available for molecular mechanics calculations for molecules such as L^1 and therefore that it should be used whenever possible. We did not have the MM2 force field available for molecular dynamics and therefore used the INSIGHT/DISCOVER software. While this does use a different force field from MM2 (as is clear from the text) we carried out different types of calculations using it in order to locate approximate conformational minima rather than to obtain accurate information about structure and energy for which we (later) used MM2MX.

Table 3 Energies (kcal mol^{-1}) obtained from the MM2MX, INSIGHT/DISCOVER and MOPAC programs for the four conformations of L^1

	MM2MX*			
Conformation	1	2	INSIGHT/ DISCOVER	MOPAC (5.0)
sss	19.86	87.42	167.57	311.7
sso	31.82	81.12	173.21	270.0
soo	22.66	79.04	169.32	265.8
ooo	22.45	64.10	167.42	244.6

All steric energies except for MOPAC heat of formations. * Without (1) or with (2) an electrostatic contribution.

Table 4 Conformation frequencies observed for L^1 during molecular dynamics runs (conditions as given in the text)

	Frequency of observation of each structure			
Starting conformation	**sss**	**sso**	**soo**	**ooo**
sss	0	0	4	46
sso	0	0	6	44
soo	0	0	6	44
ooo	0	1	22	27
Total	0	1	38	161

Table 5 Steric energies (kcal mol^{-1}) obtained from the MM2MX program[a] for the four isomers with water molecules included

		Model[b]			
Conformation	L^1	A	B	C	D
sss	87.42	85.81	79.06	69.52	*c*
sso	81.12	82.46	72.80	64.35	73.60
soo	79.04	83.26	73.64	64.39	74.59
ooo	64.10	69.07	64.76	59.70	60.86

[a] Bond dipoles used are detailed in Table 2. [b] Models are as follows (see text); A, one water molecule in the middle of the macrocycle (no hydrogen bonds formed); B, one water molecule within one end of the macrocycle with a hydrogen bond formed to the bridgehead nitrogen atoms; C, two water molecules inside, one at each end of the macrocycle, each hydrogen bonded to a bridgehead nitrogen atom; D, one water molecule outside the macrocycle forming a hydrogen bond to an imine nitrogen atom. [c] Not calculated as no hydrogen bond could be formed.

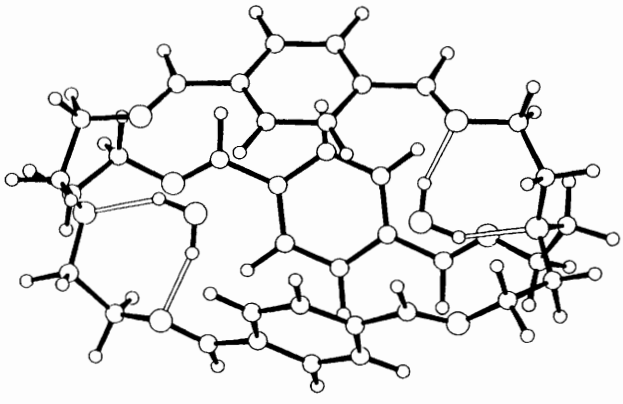

Fig. 6 The structure of conformation **soo** of L^1 with two water molecules included and hydrogen bonded to the bridgehead nitrogen atoms

distribution is particularly interesting as the energies of all four conformations were similar (**sss** 167.6, **sso** 173.2, **soo** 169.3, **ooo** 167.4 kcal mol^{-1}) when calculated using the CVFF force field[9] which was used in the dynamics. Even when the **sss** and **sso** conformations were used as the initial model the macrocycle changed to the **soo** or **ooo** conformation within the first ps. The conformation did not alternate much between the **soo** and **ooo** forms and indeed stayed at one or the other for several ps during the runs. Indeed when the time of the run with the **soo** starting conformation was extended to 100 ps we found that the **ooo** conformation observed after 50 ps remained unchanged for the next 50 ps. These results are dependent to some extent on the value of the V_2 force-constant parameter given to the N=C–C_{ar}–C_{ar} torsion angle. We chose a value of 2.5 kcal mol^{-1}. However we tested the effect of varying this value. In the molecular dynamics runs the time taken for the **sss** or **sso** conformation to change to the **soo** or **ooo** conformation was related to the value of V_2 though usually remained less than 1 ps. However the conformational frequencies (Table 4) were not much affected by changes in V_2.

The macrocycle in water. We then used these computational methods to investigate whether water molecules could be enclosed within the macrocycle. The four conformations of the macrocycle were used as starting models. Using our molecular graphics system, a water molecule was placed in the centre of the macrocycle (model A), and then one molecule at one end of the macrocycle (model B), two molecules at either end of the macrocycle (model C) and then one water molecule outside the macrocycle (model D). In each case wherever possible we formed hydrogen bonds between the hydrogen atoms on the water molecule and nitrogen atoms. Bond dipoles for the water molecule were taken directly from the MM2MX program. The hydrogen atoms on the water molecule were treated as potentially hydrogen-bond forming atoms using the parameters suggested by Allinger *et al.*[16] Results of the molecular mechanics minimizations are shown in Table 5.

For all conformations, it proved possible to place a water molecule at the centre of the macrocycle without unreasonably close contacts between host and guest, but the resulting host–guest complex had a higher energy than that of the host for all conformations apart from the **sss** but in that conformation the starting energy was particularly high. We conclude that placement of the water molecule in the centre of the macrocycle is unlikely, particularly as no hydrogen bonds could be formed.

For all four conformations, two water molecules could be fitted within the macrocycle, one at each end. In all cases a strong hydrogen bond could be formed to the bridgehead nitrogen atom. For some of the conformations it also proved possible to link the second water hydrogen atom to an imine nitrogen but the geometry for this interaction was not so favourable for hydrogen-bond formation. Attempts to form two hydrogen bonds to two imine nitrogen atoms rather than one to the bridgehead nitrogen atom and a second weak bond to an imine (Fig. 6) were unsuccessful. As can be seen from the energies of the host–guest complex, the **ooo** conformation, in which the lone pairs on the six nitrogen atoms are pointing outwards, proved the least successful in encapsulating two water molecules and only 4.40 kcal mol^{-1} of interaction energy was gained, whereas all the other three conformations gained *ca.* 15–18 kcal mol^{-1} of interaction energy. Fig. 6 shows the most favourable positions of two water molecules within the **soo** conformation. We also compared (model D) the interaction energy of the water molecule outside the macrocycle and inside the macrocycle (model B). In these cases there was little difference indicating that the water molecules would be as stable within the macrocycle as without. However this is only true if the water molecules are able to enter the macrocycle cavity. We investigated this possibility with the INSIGHT/DISCOVER software[9] by placing the molecule in the **soo** conformation within a water box of size (20 × 15 × 15 Å). A molecular dynamics run was then carried out at 300 K for 100 ps. During that time the water molecules readily moved inside and outside the macrocycle. As in the gas phase the **soo** and **ooo** conformations were favoured. On average 2.9 hydrogen bonds were formed at any one time with the vast majority

Table 6 Proton NMR data of L^1 and derivatives

Compound	T/°C	Solvent	ν/MHz	A[b]	C[b]	D[b]	E[b]
1 L^1	25	CD_3OD	360	7.32(s)	8.29(s)	3.84(t)	2.83(br s)
	−90	CD_3OD	400	7.00–7.60(br m)	8.40(s)	3.90(br m)	3.48(t), 2.06(d)
2 $[Ag^2L^1]^{2+}$	20	CD_3CN	400	7.86(s)	8.69(s)	3.89(t)	3.09(t)
	−40	CD_3CN	400	7.86(s)	8.69(s), 8.67(d)	3.86(br s)	3.05(br t)
3 $[Cu^2L^1]^{2+}$	20	CD_3CN	400	7.74(s)	8.59(s)	3.87(t)	3.15(t)
	−40	CD_3CN	400	7.72(s)	8.58(s)	3.83(br t)	3.11(5)
4 $[H^2L^1]^{2+}$	20	$(CD_3)_2SO$[c]	400	7.55(s)	8.58(br s)	4.05(br s)	3.79(br s)

[a] In ppm from $SiMe_4$. s = Singlet, d = doublet, t = triplet, m = multiplet, and br = broad. [b] The integration of these signals was in the ratio 2(A):1(C):2(D):2(E). [c] A broad signal at δ 7.04 was attributed to $NH^+ \cdots N$.

between imine nitrogen atoms and water molecules outside the macrocycle.[17]

However our calculations show that the formation of a hydrogen bond outside the macrocycle between a water molecule and an imine nitrogen is not particularly favoured. Even for the **ooo** conformation where all the imine nitrogen atoms are divergent, the placement of a water molecule outside the macrocycle hydrogen bonded to an imine nitrogen atom is only slightly favoured over a water molecule inside the macrocycle hydrogen bonded to a bridgehead nitrogen atom. Indeed the formation of a hydrogen bond outside the macrocycle is hampered by repulsions between the water molecule and the adjacent phenyl rings. This may cause an increase in the N ··· O distances and indeed the values found in the crystal structure are quite long [2.95(1) Å] for interactions of this type.

These results are consistent with the crystal structure of $L^1 \cdot 6H_2O$, in that the **ooo** conformation has the lowest energy and that for that structure the water molecules give a higher interaction energy outside, rather than inside, the macrocycle. The structure contains six water molecules per macrocycle and of course there is no way in which more than two molecules of water can fit inside the macrocycle. Outside the macrocycle, all six water molecules can form hydrogen bonds to the imine nitrogen atoms and in addition they can also form hydrogen bonds to each other (Table 1) to stabilize the crystal structure.

Protonated Salts: Disilver and Dicopper(II) *Complexes.*—It became obvious early on in our transmetallation attempts that the cryptand L^1 was well adapted to encapsulation of H^+; protonated ligand salts were obtained on treatment of L^1 with most first transition series ions in the absence of co-ordinating counter ions. Only in the case of Cu^I and Ag^I was there any effective competition with this outcome. The strength of the hydrogen bond which can be inferred from this observation, together with the low-field ^1H NMR signal and sharp ν_{NH} in the infrared spectrum, suggests that the protons are intramolecularly hydrogen bonded between the site of protonation (most likely the bridgehead nitrogen atom) and one of the imino nitrogen atoms.

Protons were placed on the bridgehead nitrogens to calculate the relative stability of the cations and also to test the likelihood of internal hydrogen-bond formation. We ran MOPAC 5.0 on the cations and found some changes in the atomic charges from those found on the free ligands. Consequently the bond dipoles for C–N(sp^3) were changed to 0.12 and N–H^+ to 0.45D. The other bond dipoles were kept the same (Table 2). These two protons were given parameters that allowed formation of hydrogen bonds.[17] Resulting energies for $[H_2$**sss**$]^{2+}$, $[H_2$**sso**$]^{2+}$, $[H_2$**soo**$]^{2+}$, $[H_2$**ooo**$]^{2+}$ were 60.49, 54.89, 54.21 and 51.47 kcal mol^{-1} respectively. It is interesting that the **ooo** conformation, while remaining that of lowest energy, now has an energy much more comparable with the other three thus indicating that the **ooo** conformation is much less favoured over the other geometries as the $2H^+$ cation than as the free ligand. Indeed MOPAC heats of formation (using the PM3 parameterization) indicate an **ooo** conformation marginally less stable

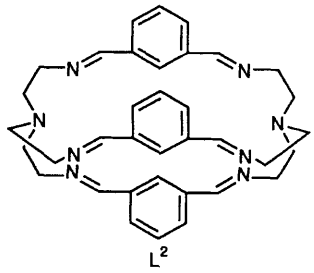

L^2

than the others ($[H_2$**sss**$]^{2+}$ 543.8, $[H_2$**sso**$]^{2+}$ 554.8, $[H_2$**soo**$]^{2+}$ 550.4, $[H_2$**ooo**$]^{2+}$ 565.6 kcal mol^{-1}).

Analysis of the H(bridgehead) ··· N(imine) distances in the cations indicated that for some conformations weak intramolecular hydrogen-bond interaction was possible although in no conformation was the geometry optimal. The most favourable geometry occurred in **soo** and **sso** conformations with H ··· N distances of 2.43–2.57 and 2.47–2.51 Å respectively compared to **sss** (2.55–2.62 Å) and **ooo** (2.63–2.64 Å).

Proton NMR spectra of L^1 in the different configurations represented by $L^1 \cdot 6H_2O$ and $[M_2L^1]^{2+}$ (M = Ag, Cu or H) are compared in Table 6. Irrespective of conformational factors, a co-ordination shift in the ^1H(C=N) signal deriving from loss of electron density upon co-ordination of the imino nitrogen atom is to be expected. Such a low-field shift is indeed found for the dicopper(I) and, more noticeably, disilver(I) cryptates, although this may be modified by conformational effects which we are unable to quantify. It is interesting that the ^1H(C=N) signal of $[Ag_2L^1]^{2+}$ splits into two components of equal intensity at the lowest temperature accessible in CD_3CN. The 8 Hz doublet separation is independent of spectrometer frequency (at 300, 400 and 500 MHz) and so must be attributed to a coupling process. No splitting of the ^1H(C=N) signal is seen for the isostructural $[Cu_2L^1]^{2+}$, and indeed a similar 8–10 Hz splitting appears in the low-temperature spectrum of other disilver [but not dicopper(I)] cryptates we have studied.[8] The most likely explanation of the splitting is therefore a $^3J(^1H-^{109,107}Ag)$ coupling; the sample was insufficiently soluble to permit any attempt at direct conformation *via* ^{109}Ag NMR spectroscopy. Presumably rapid exchange of Ag^+ between cryptand and solvent explains the loss of coupling at ambient temperature.

The aromatic signal of $[M_2L^1]^{2+}$ (M = Cu, Ag or H) shifts downfield at 0.4–0.5 ppm relative to the free ligand. As no co-ordination shift is to be expected in this case, conformational effects, most likely additional deshielding from the ring currents of the trigonally disposed neighbouring aromatic rings, must be invoked to explain the shifts. In contrast to the situation in the isomeric *meta*-cyclophane, L^2, no anomalous chemical shift values such as those deriving[18] from close approach of aromatic rings in L^2 were observed. However, as in L^2, fluxionality arising from differentiation of the methylene CH_2 protons into H_{ax} and H_{eq} is evident at low temperature. Coalescence temperatures for the L^1 methylene signals are significantly lower than with L^2, as may be expected from the lesser degree of steric constraint anticipated for this larger cryptand. By

−80 °C, H_E has separated into two signals, a broad doublet (H_{eq}) at δ 2.06 and a poorly resolved triplet (H_{ax}) at δ 3.48. while H_D presents a poorly resolved multiplet, apparently not far from coalescence. The large (≈1.42 ppm) separation of H_E axial and equatorial signals may reflect involvement of the equatorial proton in shielding by the anisotropic circulation of more than one aromatic ring. Fig. 2 illustrates the relative disposition of the H_E equatorial protons with respect to the aromatic rings. Unfortunately the low coalescence temperature and consequent poorly resolved 'soft' nature of the spectra at −80 °C prevents use of nuclear Overhauser enhancement (NOE) further to investigate through-space relationships, as was done [18] for L^2.

As the cryptates $[Ag_2L^1][CF_3SO_3]_2$ **2** and $[Cu_2L^1][CF_3SO_3]_2$·EtOH **3** are soluble only in polar solvents such as acetonitrile, the methylene signals are merely broadened at the lowest temperature (≈40 °C) available. The broadening in this case is more evident in the H_D triplet, the H_E signal being only marginally affected. Methylene signals are sensitive to conformation in this Schiff-base cryptand series, particularly in respect [19] of the relative position and separation of axial and equatorial signals. It is unfortunate that we are unable to obtain the 'frozen-out' spectrum for **2** and **3** as X-ray crystallographic data, available for L^3 in both cryptand and cryptate form, which would assist our rationalization of the chemical shift.

The diprotonated salt $[H_2L^1][ClO_4]_2$ **4** is soluble only in dimethyl sulphoxide, which severely limits the available temperature range. At ambient temperature all signals are broad and no coupling is resolved. The imino and aromatic protons are assigned on the basis of intensity and the methylene signals now appear close together at δ 4.05 and 3.79. The ≈1 ppm downfield shift of the H_E signal represents a significant deshielding, which presumably derives from proximity to the NH^+ protonation site. (There is some indirect evidence in favour of an intramolecular hydrogen bond, in that irradiation into the hydrogen-bond signal at δ 7.04 generates a similar NOE of both methylene signals.) The broadening of these signals may arise from exchange of hydrogen-bond acceptor sites among the imino nitrogens. Modelling studies have shown that N–H ••• N geometries are similar for all three sites.

At the lowest temperature achieved for L^1 in CD_3OD the aromatic signal has split into several broad components. As many as seven separate signals can be discerned in the broad envelope, suggesting that the more abundant conformations may be unsymmetric. Our inability further to reduce the temperature prevents analysis of this interesting spectrum.

Transition-metal Complexes.—Despite the ease of formation of disilver(I) complexes, L^1 showed considerable reluctance to accommodate transition-metal ion guests except in the presence of further ligands. Dicopper(I) complexes were, however, readily obtained on treatment of L^1 with salts of either Cu^I or Cu^{II}, in keeping with electrochemical results [20] which indicate borderline Cu^I/Cu^{II} stability. The ditriflate salt **3** was obtained by slow evaporation of the green solution obtained by mixing L^1 with $Cu(CF_3SO_3)_2$ in ethanol; the rapid-precipitation strategy (L^1 in CH_2Cl_2, Cu^{2+} in EtOH) which succeeded in generating $Cu_2^{II}(\mu\text{-}OH)^{3+}$ complexes of related cryptands [19] in this case resulted in precipitation of the diprotonated salt **4**. The X-ray diffraction pattern of the bronze crystals **3** was identical with that of the structurally characterized complex **2**, so the copper(I) co-ordination site can be inferred to be the distorted tetrahedron revealed [8] for Ag^I. Evidently the co-ordination preferences of Cu^I rather than Cu^{II} are satisfied by the site presented in the convergent (**sss**) form of L^1.

We checked whether the four conformations could accommodate cationic guests at either end of the molecule. In the $[AgL^1]^{2+}$ structure the silver atoms are positioned inside the macrocycle, one at each end and bonded to four nitrogen atoms each. The macrocycle has the **sss** conformation where all the imine nitrogen atoms are convergent. This structure has one peculiarity in that both silver atoms have close contacts with three *ortho*-hydrogen atoms from the bridging phenyl rings. These Ag ••• H distances are 2.72, 2.65 and 2.52 Å for one silver and 2.37, 2.32 and 2.26 Å for the other. It is likely that these distances represent some kind of interaction. The short Ag ••• H contact may result from steric necessity rather than any weak bonding interaction, though a molecular mechanics calculation using appropriate van der Waals constants for metal and hydrogen atoms led to a minimum-energy structure in which the metal–metal distance was 7.39 rather than the 6.06 Å actually found.[8]

These close M ••• H interactions are presumably a cause of instability and indicate the reason why it is difficult to encapsulate metal ions within the macrocycle. Another reason is that the resulting geometry is very distorted in that all four nitrogen atoms are on one side of the silver atom, an unlikely arrangement for many transition metals.

If all four nitrogen donors are to be used, two metals can be encapsulated only in the **sss** conformation. In the other three conformations, the four nitrogen atoms are not in suitable positions for simultaneous binding. In the **ooo** conformation there is no chance of encapsulating the metal ion as all the lone pairs on the imine nitrogen atoms are divergent, pointing away from the macrocycle cavity. In the **soo** and **sso** conformations a metal atom can be bonded to a bridgehead nitrogen atom, but then to only two of the three imine nitrogen atoms as the lone pair on the third nitrogen atom is directed away from the metal atom. Remaining co-ordination positions could then be filled by non-macrocyclic ligands.

Infrared spectra (Table 7) indicate that the thiocyanate ligand is terminally N-bonded rather than bridging. (Attempts to incorporate the two- or three-atom bridges pyrazolate or imidazolate were unsuccessful.) The electronic spectrum of $[Cu_2L^1(NCS)_4]$·$2H_2O$ **5** shows a single broad d–d absorption in the far red/near infrared consistent with four-co-ordination of Cu^{II}. The ESR spectrum, run as dimethylformamide (dmf) glass, takes the form of an axial four-line signal ($g_\perp$ = 2.08, $g_\parallel$ = 2.33) with normal $A_\parallel$ hyperfine splitting of 147 G (1.47×10^{-2} T). No half-band signal can be seen at up to 20 times the sensitivity used for the main band signal. Clearly no strong interaction exists between these fairly widely separated unbridged paramagnets, a finding supported by magnetic susceptibility measurements over the temperature range 80–300 K.

The cryptand L^1 was also treated with Co^{II} and Ni^{II} in the presence of thiocyanate ion. Electronic spectra and magnetic susceptibility measurements for $[Co_2L^1(NCS)_4]$·$3H_2O$ **6** and $[NiL^1(NCS)_4]$·$4H_2O$ **7** show that the co-ordination site is a reasonably good approximation to tetrahedral, so the donor set contains no more than two of the possible four cryptand N-donors in addition to the pair of N-terminal thiocyanates. Splitting of the ν(C=N) imino absorption into two components (often poorly resolved) supports the idea that not all imine donors are co-ordinated which indeed was the implication of the molecular mechanics simulations.

A bis(thiocyanate) complex $[Ni_2L^1(NCS)_2][ClO_4]_2$ **8** was obtained, in the case of Ni^{II} only. Neither electronic spectral nor magnetic measurements support tetrahedral co-ordination in this case and five- or possibly six-*co-ordination may be assumed, with N-terminal NCS^- complementing the cryptand donors. The temperature dependence of the magnetic susceptibility for **6**–**8** is no more than expected for an isolated Ni^{2+} or Co^{2+} ion, so cannot be taken as evidence of interaction between neighbouring paramagnetic centres. This is so even in the case of **6** which has the $^4A_2$ ground state which facilitates superexchange when a bridging donor atom is present.[21] Geometric constraints within the cryptand apparently prevent accommodation of the thiocyanate ligand in a 1,3-bridging

* Some broadening of the ClO_4 ν_3 absorption may indicate weak co-ordination of this counter ion.

Table 7 Infrared and electronic spectral and magnetic susceptibility data

Complex	Colour	d–d absorptions $\tilde{\nu}_{max}$	ε	IR data (cm^{-1}) ν(C=N)	ν_{asym}(NCS)	μ^b (K) 300	80
5 $[Cu_2L^1(NCS)_4]$	Dark olive-green	13 500	145	1634ms 1622ms	2075vs 2037ms	2.01	1.92
6 $[Co_2L^1(NCS)_4]\cdot 3H_2O$	Blue	16 050 7 030	600 100	1642ms 1620(sh)	2059vs	4.5	4.2
7 $[Ni_2L^1(NCS)_4]\cdot 4H_2O$	Blue-green	16 130 8 400	45 102	1628ms 1610(sh)	2063vs	3.7	3.4
8 $[Ni_2L^1(NCS)_2][ClO_4]_2$	Deep pink	18 020mw[c] 11 000vw 26 300(sh)		1638ms 1610(sh)	2070s	3.2	2.9

[a] 10^{-3} mol dm^{-3} in dimethylacetamide, $\tilde{\nu}$ in cm^{-1}, ε in cm^2 mol^{-1}. [b] Per metal ion. [c] Insoluble; Nujol mull spectrum.

mode; although the internuclear distance is of the right order for such a bridge, the preferred *ca.* 180° M–N–C and *ca.* 90° C–S–M angles are more difficult to accommodate. The μ-1,3-N_3^- bridge is less sterically demanding, but attempts at synthesis of analogous tetraazido complexes led only to impure and insoluble products whose $\nu_{asym}(N_3^-)$ infrared absorption appears in the region normally associated[22] with terminal co-ordination.

The octaamino derivative L^3 (= L^1 + 12H) which will be the subject of a subsequent paper offers enhanced flexibility to the co-ordination site. This increases the chance of successful competition for the co-ordination site by transition-metal ion *versus* H^+ and also the likelihood of eventual incorporation of bridging ligands between the co-ordination transition-metal ion guests.

Experimental

$L^1\cdot 6H_2O$ **1**.—Terephthalaldehyde (3 mmol) and tren (2 mmol) were stirred in MeCN (100 cm^3) at ambient temperature for 3–4 h. The crude yellowish product was filtered off and recrystallized from methanol. Colourless cubes were obtained in 40–60% yield (Found: C, 61.7; H, 7.9; N, 16.5. Calc.: C, 62.1; H, 7.8; N, 16.1%).

$[Ag_2L^1][CF_3SO_3]_2$ **2**.—To a solution of $AgNO_3$ (2 mmol) in MeOH (100 cm^3) at 50 °C was added terephthalaldehyde (3 mmol) and tren (2 mmol). The mixture was stirred for 2 h at 50 °C, filtered and concentrated. Following addition of excess of $Li(CF_3SO_3)$, the mixture was left to crystallize in the dark when yellow crystals were obtained in 89% yield (Found: C, 41.3; H, 3.9; N, 10.2. Calc.: C, 41.5; H, 3.4; N, 10.5%).

$[Cu_2L^1][ClO_4]_2$ **3′**.—To compound **1** (0.2 mmol) dissolved in deoxygenated CH_2Cl_2 (30 cm^3) was added $[Cu(MeCN)_4]$-ClO_4 (0.4 mmol) in MeCN (20 cm^3) and the solution was concentrated to ≈ 20 cm^3. Bronze crystals were obtained in 55% yield (Found: C, 47.2; H, 4.6; N, 12.2. Calc.: C, 47.4; H, 4.6; N, 12.3%).

$[Cu_2L^1][CF_3SO_3]_2\cdot$EtOH **3**. The salt $Cu(CF_3SO_3)_2$ (0.4 mmol), dissolved in MeCN (100 cm^3) was added to a solution of **1** (0.2 mmol) in EtOH (100 cm^3). The resulting green solution was stirred for 3 h at 40–45 °C, filtered and reduced in volume. Bronze crystals were obtained on slow evaporation (Found: C, 47.7; H, 4.7; N, 11.0. Calc.: C, 47.2; H, 4.8; N, 11.4%).

$[H_2L^1][ClO_4]_2$ **4**.—The protonated derivative was obtained as the product of attempted template synthesis of compound **1** on copper(II). Thus tren (0.2 mmol), terephthalaldehyde (0.3 mmol) and $Cu(ClO_4)_2\cdot 6H_2O$ (0.2 mmol) were stirred in an EtOH–MeCN solvent mixture for 0.5 h at ambient temperature. The solution rapidly became turbid and the finely crystalline colourless product was filtered off. A second crop was obtained on standing (Found: C, 54.4; H, 5.6; N, 13.9. Calc.: C, 54.4; H, 5.5; N, 14.1%).

$[Cu_2L^1(NCS)_4]\cdot 2H_2O$ **5**.—The salt $Cu(CF_3SO_3)_2$ (0.33 mmol) in cold MeCN (30 cm^3) was added to a cold mixture of **1** (0.17 mmol) and NaNCS (0.74 mmol) dissolved in EtOH (40 cm^3). The initial olive-green powder was filtered off and the filtrate left overnight in a freezer when small dark green crystals were obtained. If the solution is allowed to warm or is left too long before filtration the green copper(II) product is contaminated with the orange copper(I) salt (Found: C, 48.4; H, 4.3; N, 17.1. Calc.: C, 48.9; H, 4.7; N, 17.5%).

$[Co_2L^1(NCS)_4]\cdot 3H_2O$ **6**. Compound **1** (0.17 mmol) in EtOH (30 cm^3) was added to a mixture of $Co(ClO_4)_2\cdot 6H_2O$ (0.33 mmol) and NaNCS (0.7 mmol) in MeCN (40 cm^3) at ambient temperature. Turbidity soon developed and the solution was stirred for 0.5 h before filtering off the blue powder in 75% yield. The product could be recrystallized from dimethylacetamide–Et_2O (Found: C, 48.5; H, 4.7; N, 16.7. Calc.: C, 48.5; H, 4.9; N, 16.9%).

$[Ni_2L^1(NCS)_4]\cdot 4H_2O$ **7**.—To $Ni(NO_3)_2\cdot 4H_2O$ (0.33 mmol) in EtOH (50 cm^3) was added NaNCS (0.7 mmol) in MeCN (20 cm^3) and **1** (0.2 mmol) in EtOH (40 cm^3) at 50 °C. The solution was stirred at 50 °C for 2 h before filtering off the blue-green product in 75% yield. It was very insoluble and could not be satisfactorily recrystallized. In several preparations a low %C value was obtained (Found: C, 46.2; H, 4.6; N, 16.6. Calc.: C, 47.6; H, 5.0; N, 16.6%).

$[Ni_2L^1(NCS)_2][ClO_4]_2$ **8**. To $Ni(ClO_4)_2\cdot 6H_2O$ (0.33 mmol) was added NaNCS (0.33 mmol) in MeCN (20 cm^3) and **1** (0.17 mmol) in EtOH (40 cm^3) at 50 °C. The initial precipitate of protonated L^1 perchlorate salt was filtered off and the blue filtrate slowly evaporated to yield purple-pink crystals (Found: C, 45.0; H, 4.0; N, 13.6. Calc.: C, 44.8; H, 4.1; N, 13.7%).

Physical Measurements.—Electronic and ESR spectra were measured using PEλ9 and Varian E109 spectrometers; magnetic susceptibility measurements were made with an Oxford Instruments Faraday susceptibility system as described earlier.[22]

Crystal Structure Determination of $L^1\cdot 6H_2O$.—*Crystal data.* $C_{36}H_{54}N_8O_6$, M = 694.4, rhombohedral (hexagonal setting), space group $R32$, a = 14.834(14), c = 15.594(16) Å, U = 2971.7 $Å^3$, $F(000)$ = 1122, D_m = 1.14 g cm^{-3}, Z = 3, D_c = 1.17 g cm^{-3}, Mo-Kα radiation (λ = 0.710 7 Å), μ(Mo-Kα) = 0.87 cm^{-1}.

A crystal of approximate size 0.3 × 0.4 × 0.2 mm was set up to rotate about the {120} axis on a Stoe STADI2 diffractometer and data were collected *via* variable-width ω scans. Background counts were for 20 s and a scan rate of 0.0333° s^{-1} was applied to

Table 8 Atomic coordinates ($\times 10^4$) with estimated standard deviations in parentheses for $L^1 \cdot 6H_2O$

Atom	x	y	z
N(1)	0	0	3378(3)
C(0)	544(4)	1095(3)	3686(2)
C(1)	1593(4)	1764(4)	3279(3)
N(2)	1486(3)	1964(3)	2369(2)
C(3)	1875(3)	1637(3)	1821(3)
C(4)	1836(3)	1733(3)	890(3)
C(5)	1381(4)	2249(4)	520(3)
C(6)	1320(4)	2281(4)	−363(3)
O(7)	359(4)	3130(5)	2433(3)

Table 9 Molecular dimensions (distances in Å, angles in °)

N(1)–C(0)	1.486(4)	N(1)–C(0)–C(1)	113.7(3)
C(0)–C(1)	1.505(6)	C(0)–N(1)–C(0^{II})	110.1(4)
C(1)–N(2)	1.474(6)	C(0)–C(1)–N(2)	111.0(4)
N(2)–C(3)	1.257(6)	C(1)–N(2)–C(3)	117.4(4)
C(3)–C(4)	1.463(6)	N(2)–C(3)–C(4)	126.1(4)
C(4)–C(5)	1.375(6)	C(3)–C(4)–C(5)	121.7(4)
C(4)–C(6^{I})	1.375(6)	C(3)–C(4)–C(6)	119.9(4)
C(5)–C(6)	1.382(6)	C(5)–C(4)–C(6)	118.4(4)
		C(4)–C(5)–C(6)	119.7(6)
		C(4)–C(6^{I})–C(5^{I})	121.8(6)

Symmetry elements: I $y, x, -z$; II $-y, x-y, z$

Table 10 Torsion angles (°) in L^1 (**ooo** conformation as found in the crystal structure of $L^1 \cdot 6H_2O$) and the **sss** conformation as found in the crystal structure of $[Ag_2L^1]^{2+}$

		sss		
	ooo			
N(1)–C(*n*0)–C(*n*1)–N(*n*2)	70.2	48.8	54.4	52.8
C(*n*0)–C(*n*1)–N(*n*2)–C(*n*3)	−118.1	128.3	139.3	135.3
C(*n*1)–N(*n*2)–C(*n*3)–C(*n*4)	−178.6	174.4	170.8	−179.3
N(*n*2)–C(*n*3)–C(*n*4)–C(*n*5)	2.6	−24.2	−22.4	−27.7
C(*n*3)–C(*n*4)–C(*n*5)–C(*n*6)	−177.1	−178.5	175.9	−177.2
C(*n*5)–C(*n*6)–C(*n*7)–C(*m*0)	*	178.7	−178.4	−178.2
C(*n*6)–C(*n*7)–C(*m*0)–N(*m*1)	*	19.5	26.7	7.6
C(*n*7)–C(*m*0)–N(*m*1)–C(*m*2)	*	171.5	172.5	176.1
C(*m*0)–N(*m*1)–C(*m*2)–C(*m*3)	*	147.4	136.3	142.0
N(*m*1)–C(*m*2)–C(*m*3)–N(1)	*	61.7	54.9	57.4

* Equivalent to a previously quoted angle by symmetry.

a width of (1.5 + sin μ/tan θ). 1751 Reflections with $2\theta_{max}$ of 50° were measured on a Stoe STADI2 diffractometer, of which 1065 were independent and 973 with $I > 2\sigma(I)$ were used in subsequent calculations. The structure was solved by direct methods. The cation had crystallographically imposed 32 symmetry so only 1/6 of the molecule was independent. All non-hydrogen atoms were given anisotropic thermal parameters. Hydrogen atoms were placed in calculated positions apart from those on the water molecule. Only one hydrogen could be located in a Fourier difference map on this atom and this was refined independently. Data were given a weighting scheme in the form $w = 1/[\sigma^2(F) + 0.003F^2]$. The final R value was 0.090 ($R' = 0.092$). We were unable to differentiate between enantiomorphs.

Calculations were carried out using SHELX 76[23] and some of our own programs on the Amdahl 5780 computer at the University of Reading. In the final cycles of refinement no shift/error ratio was greater than 0.1σ. In the final Fourier difference maps the maximum and minimum peaks were 0.25 and −0.36 e Å^{-3} respectively. Positional parameters are given in Table 8, molecular dimensions in Table 9, torsion angles in Table 10 and details of the hydrogen bonding in Table 1.

Additional material available from the Cambridge Crystallographic Data Centre comprises H-atom coordinates and thermal parameters.

Acknowledgements

We thank the Department of Education for Northern Ireland, Du Pont (UK) and the Open University Research Committee for support. The help of the SERC services at Swansea (fast atom bombardment mass spectrometry) and Warwick (high-field NMR spectroscopy) is gratefully acknowledged. Thanks are also due to Mr. A. Johans for assistance with the crystallographic measurements.

References

1 J.-M. Lehn, *Acc. Chem. Res.*, 1978, **11**, 49.
2 J.-M. Lehn, *Pure Appl. Chem.*, 1980, **52**, 2441.
3 J.-M. Lehn, *Angew. Chem., Int. Ed. Engl.*, 1988, 2139.
4 J. Castro, J. Romero, J. A. Garcia-Vasquez, M. Duran, A. Castineiras, A. Sousa and D. E. Fenton, *J. Chem. Soc., Dalton Trans.*, 1990, 3255 and refs. therein.
5 S. M. Nelson, *Pure Appl. Chem.*, 1980, **52**, 2461.
6 J. Jazwinski, J.-M. Lehn, D. Lilienbaum, R. Ziessel, J. Guilheim and C. Pascard, *J. Chem. Soc., Chem. Commun.*, 1987, 1691.
7 D. McDowell and J. Nelson, *Tetrahedron Lett.*, 1988, 385.
8 M. G. B. Drew, D. McDowell and J. Nelson, *Polyhedron*, 1988, **12**, 2229.
9 INSIGHT/DISCOVER, Insight II version 2.0.0, Discover version 2.7.0, CVFF forcefield, Biosym. Inc., San Diego, CA, 1991.
10 MM2MX program contained with the RIPS program QCPE No. 588, D. M. Ferguson and D. J. Raber, Quantum Chemistry Program Exchange, Chemistry Department, Indiana University, IN, QCPE 395 and based on N. L. Allinger and Y. H. Yuh , MM2(77), 1989.
11 MOPAC version 5.0, J. J. P. Stewart, QCPE No. 455, Quantum Chemistry Program Exchange, Chemistry Department, Indiana University, IN, 1990.
12 J. R. Damewood, W. D. Anderson and J. J. Urban, *J. Comput. Chem.*, 1988, **9**, 111.
13 M. G. B. Drew and A. Santos, *J. Chem. Soc., Faraday Trans.*, 1991, **87**, 1321.
14 N. L. Allinger, personal communication, 1990
15 J. J. P. Stewart, *J. Comput. Chem.*, 1989, **10**, 209, 220.
16 N. L. Allinger, R. A. Kok and M. R. Iman, *J. Comput. Chem.*, 1988, **9**, 591.
17 M. G. B. Drew, unpublished work.
18 V. McKee, W. T. Robinson, D. McDowell and J. Nelson, *Tetrahedron Lett.*, 1989, **30**, 7453.
19 D. Marrs, Ph.D. Thesis, Open University, 1990.
20 M. McCann and J. Nelson, unpublished work.
21 M. G. B. Drew, F. S. Esho, A. Lavery and S. M. Nelson, *J. Chem. Soc., Dalton Trans.*, 1984, 545.
22 C. J. Harding, D. Marrs, J. Nelson, S. Raghunathan, C. Stevenson, P. C. Yates and M. G. B. Drew, *J. Chem. Soc., Dalton Trans.*, 1990, 2521.
23 SHELX 76, Package for Crystal Structure Determination, G. M. Sheldrick, University of Cambridge, 1976.

Received 19*th April* 1991; *Paper* 1/01846I